Critical-noise measurement near Fréedericksz transitions in nematic liquid crystals

P. Galatola and M. Rajteri
Dipartimento di Fisica del Politecnico di Torino, Corso Duca degli Abruzzi 24, 10129 Torino, Italy
(Received 10 June 1993)

We present a dynamic light-scattering experiment on a planarly oriented nematic liquid crystal in the presence of a symmetry-breaking electric field applied normally to the cell planes. This experiment gives direct evidence for the critical behavior of the lowest splay fluctuation mode. A detailed theoretical analysis of the dynamics of this mode is worked out and compared with the experimental results.

PACS number(s): 61.30.Gd, 64.70.Md, 78.35.+c

I. INTRODUCTION

Light-scattering experiments are very powerful tools for the determination of many physical parameters of nematic liquid crystals [1–6]. Recently they have also been proposed as a way to measure the surface anchoring energies [7] and to determine the threshold of the magnetically induced bend Fréedericksz transition in a homeotropic sample [8]. The latter measurements are based on the softening of some lowest-order fluctuation mode in a second-order transition induced by a symmetry-breaking external field.

In this paper we experimentally analyze a similar critical behavior in the case of the electrically induced splay Fréedericksz transition in a planarly oriented sample [9]. This situation is more delicate from the experimental point of view, since it requires a forward nondepolarized scattering geometry.

In Sec. II we give a detailed analysis of the dynamics of the transversally homogeneous fluctuation modes in a nematic-liquid-crystal sample with strong planar anchoring in the presence of a destabilizing electric field, and in particular we determine approximate analytical expressions for the relaxation constant and the amplitude of the lowest-order critical splay mode. In Sec. III these results are compared with the experimental data obtained by measuring the noise power spectrum of the scattered light under heterodyne conditions: this allows one to determine the critical field and, through the knowledge of the dielectric anisotropy, the splay elastic constant and a suitable viscosity coefficient. Our results are summarized in Sec. IV.

II. THEORY

Let us consider a nematic-liquid-crystal (NLC) cell confined between the planes $z = \pm d/2$ of a Cartesian coordinate system. The director $\mathbf{n}$ undergoes small thermal fluctuations around its uniform planar orientation, imposed by strong surface boundary conditions, $\mathbf{n} = \hat{\mathbf{x}}$, $\hat{\mathbf{x}}$ being the unit vector parallel to the x axis, and is subject to a dielectric coupling with the electric field generated by the external voltage V applied to the cell. By restricting ourselves to fluctuation modes that are homogeneous in the transverse directions x and y and neglecting terms of order higher than two in the fluctuations, the free energy $\mathcal{F}$ of the NLC can be expressed as [10,11]

$$\mathcal{F} = \frac{1}{2}\int \theta^t \mathcal{L}\theta \, d\mathbf{r} \,, \tag{2.1}$$

where θ is the column matrix of the fluctuations of the director components

$$\theta = \begin{pmatrix} n_z \\ n_y \end{pmatrix} \,, \tag{2.2}$$

θ^t is the transpose of θ, and $\mathcal{L}$ is the matrix self-adjoint operator

$$\mathcal{L} = \begin{pmatrix} -K_1 \dfrac{\partial^2}{\partial z^2} - \epsilon_0 \epsilon_a \left(\dfrac{V}{d}\right)^2 & 0 \\ 0 & -K_2 \dfrac{\partial^2}{\partial z^2} \end{pmatrix} \,, \tag{2.3}$$

K_1 (K_2) being the splay (twist) elastic constant, ϵ_0 the free-space permittivity, and ϵ_a the dielectric anisotropy of the NLC, that we suppose to be positive.

The eigenvectors of the self-adjoint linear operator $\mathcal{L}$ define the static normal modes of fluctuations: when properly normalized they form a complete orthonormal set and, thanks to the equipartition theorem, their square mean amplitude in thermal equilibrium is inversely proportional to the corresponding eigenvalues. However, due to backflow effects, the dynamic fluctuation modes, and their associated decay constants, that are the actual measurable physical quantities, generally differ from the static modes, as has been shown by considering some particular cases [7].

In order to discuss the dynamics of the fluctuations, we start from the Rayleigh dissipation function for incompressible nematic liquid crystals [12,13],

$$D = \frac{1}{2}\eta_1 \frac{\partial v_\beta}{\partial x_\alpha}\frac{\partial v_\delta}{\partial x_\gamma} n_\alpha n_\beta n_\gamma n_\delta + \frac{1}{2}\eta_2 \left(n_\beta \frac{\partial v_\beta}{\partial x_\alpha} + \dot{n}_\alpha\right)\left(n_\gamma \frac{\partial v_\alpha}{\partial x_\gamma} - \dot{n}_\alpha\right)$$
$$+\frac{1}{4}\eta_3 \left(n_\beta \frac{\partial v_\beta}{\partial x_\alpha} + \dot{n}_\alpha\right)\left(n_\gamma \frac{\partial v_\gamma}{\partial x_\alpha} + \dot{n}_\alpha\right)$$
$$+\frac{1}{4}\eta_4 \left(\frac{\partial v_\beta}{\partial x_\alpha}\frac{\partial v_\beta}{\partial x_\alpha} + \frac{\partial v_\beta}{\partial x_\alpha}\frac{\partial v_\alpha}{\partial x_\beta}\right) + \frac{1}{4}\eta_5 \left(n_\beta \frac{\partial v_\alpha}{\partial x_\beta} - \dot{n}_\alpha\right)\left(n_\gamma \frac{\partial v_\alpha}{\partial x_\gamma} - \dot{n}_\alpha\right) , \tag{2.4}$$

where the Greek indices take the values x, y, z and summations over repeated indices are implied; the n_α (v_α) are the Cartesian components of the director (velocity) field; $\dot{n}_\alpha$ indicates the total derivative of n_α with respect to the time; finally the η_i ($i = 1, \ldots, 5$) are viscosity parameters that are related to the Leslie viscosity coefficients by the relations [14,15]

$$\eta_1 = \alpha_1 , \tag{2.5a}$$
$$\eta_2 = \alpha_2 + \alpha_5 = \alpha_6 - \alpha_3 , \tag{2.5b}$$
$$\eta_3 = \alpha_3 + \alpha_6 , \tag{2.5c}$$
$$\eta_4 = \alpha_4 , \tag{2.5d}$$
$$\eta_5 = \alpha_5 - \alpha_2 . \tag{2.5e}$$

By neglecting the inertia of the NLC [16], the equations of motion of the velocity field are given by

$$\frac{\partial p}{\partial x_\alpha} = \frac{\partial}{\partial x_\beta}\sigma_{\beta\alpha} , \tag{2.6}$$

where $\sigma_{\beta\alpha}$ are the components of the stress viscous tensor

$$\sigma_{\beta\alpha} = \frac{\partial D}{\partial\left(\frac{\partial v_\alpha}{\partial x_\beta}\right)} , \tag{2.7}$$

and the pressure p is implicitly determined by the incompressibility condition

$$\frac{\partial v_\alpha}{\partial x_\alpha} = 0 . \tag{2.8}$$

The equations of motion of the director field are easily determined by equating the variation of the free energy for an arbitrary infinitesimal variation of the director profile to the work done by the generalized frictional forces associated to the dissipation function D. Therefore in a linearized treatment, for $n_x \approx 1$, $n_y, n_z \ll 1$, using the expression (2.1), they read

$$\mathcal{L}\begin{pmatrix} n_z \\ n_y \end{pmatrix} = \begin{pmatrix} -\frac{\partial D}{\partial \dot{n}_z} \\ -\frac{\partial D}{\partial \dot{n}_y} \end{pmatrix} . \tag{2.9}$$

In terms of the normalized parameters

$$\zeta = \frac{\pi}{d} z , \quad \tau = \frac{K_1}{\gamma_1}\left(\frac{\pi}{d}\right)^2 t , \tag{2.10a}$$

$$w = \frac{\gamma_1 d}{\pi K_1} v_x , \quad v = \frac{1}{\pi}\sqrt{\frac{\epsilon_0 \epsilon_a}{K_1}}\, V , \tag{2.10b}$$

$$\mu_3 = \frac{\alpha_3}{\gamma_1} , \quad \mu_b = \frac{\alpha_3 + \alpha_4 + \alpha_6}{2\gamma_1} , \tag{2.10c}$$

$$r = \frac{K_2}{K_1} , \tag{2.10d}$$

where γ_1 is the rotational viscosity,

$$\gamma_1 = \alpha_3 - \alpha_2 , \tag{2.11}$$

Eqs. (2.6), (2.8), and (2.9), after linearization, split in a single equation for the y component of the director fluctuations, associated to twist deformations

$$r\frac{\partial^2 n_y}{\partial \zeta^2} = \frac{\partial n_y}{\partial \tau} , \tag{2.12}$$

and to a pair of coupled equations, associated to splay modes, for the z component of the director fluctuations and for the x component of the velocity field, that is, the only nonzero component of the velocity,

$$\left(\frac{\partial^2}{\partial \zeta^2} + v^2\right) n_z = \frac{\partial n_z}{\partial \tau} + \mu_3 \frac{\partial w}{\partial \zeta} , \tag{2.13a}$$

$$\mu_b \frac{\partial^2 w}{\partial \zeta^2} + \mu_3 \frac{\partial^2 n_z}{\partial \zeta \partial \tau} = 0 . \tag{2.13b}$$

The normal modes are defined as those solutions of the dynamic equations satisfying the strong boundary conditions

$$n_y(\zeta = \pm\pi/2) = n_z(\zeta = \pm\pi/2) = w(\zeta = \pm\pi/2) = 0 \tag{2.14}$$

that preserve their spatial profile during their temporal evolution. For the twist modes, from Eq. (2.12) we then easily obtain

$$n_y(\zeta, \tau; m) = f_m(\zeta)\exp(-\lambda_m \tau) . \tag{2.15}$$

where, up to a normalization constant,

$$f_m(\zeta) = \cos(m\zeta) , \quad m = 1, 3, 5, \ldots \tag{2.16}$$

for the even modes (with respect to the plane $\zeta = 0$), and

$$f_m(\zeta) = \sin(m\zeta) , \quad m = 2, 4, 6, \ldots \tag{2.17}$$

for the odd modes. The decay constants λ_m are given by

$$\lambda_m = r m^2 . \tag{2.18}$$

In this case, due to the absence of backflow, the dynamic modes coincide with the eigenvectors of the free energy

operator (2.3) and their (unnormalized) decay constants are equal to the corresponding eigenvalues of the free energy operator divided by the rotational viscosity γ_1. Moreover, as is evident, these modes are not affected by the applied electric field and their square mean amplitude in thermal equilibrium is easily determined from the equipartition theorem and turns out to be inversely proportional to the decay constants λ_m.

The splay modes, instead, are generally accompanied by a backflow that reduces the effective viscosity, and can be divided in solutions that are even (odd) in the director profile and odd (even) in the velocity profile. Precisely, from Eqs. (2.13), we get

$$n_z(\zeta,\tau;m) = f_m(\zeta)\exp(-\lambda_m\tau)\ , \tag{2.19a}$$

$$w(\zeta,\tau;m) = g_m(\zeta)\exp(-\lambda_m\tau)\ , \tag{2.19b}$$

where, again up to a normalization constant, for the modes even (odd) in the director (velocity) profile we have

$$f_m(\zeta) = \cos(q_m\zeta) - \cos(q_m\pi/2)\ , \tag{2.20a}$$

$$g_m(\zeta) = \frac{\lambda_m\mu_3}{q_m\mu_b}\sin(q_m\zeta) - \left(\frac{q_m^2}{\mu_3} + \frac{\lambda_m\mu_3}{\mu_b}\right)\cos(q_m\pi/2)\,\zeta\ , \tag{2.20b}$$

$$\lambda_m = \frac{q_m^2 - v^2}{1-\mu}\ , \tag{2.20c}$$

μ being the backflow parameter

$$\mu = \frac{\mu_3^2}{\mu_b}\ , \tag{2.21}$$

and q_m normalized wave vectors that are solutions of the characteristic equation

$$\cot(q_m\pi/2) = \frac{2\mu(q_m^2 - v^2)}{\pi q_m(q_m^2 - \mu v^2)}\ . \tag{2.22}$$

Since the rotational viscosity γ_1, the Miesowicz viscosity coefficient $\eta_b = \gamma_1\mu_b$ [17], and the decay constants (2.20c) at zero voltage must all be positive quantities, it immediately follows that the backflow parameter must be greater than or equal to zero and less than one.

For the splay modes odd (even) in the director (velocity) profile we have instead

$$f_m(\zeta) = \sin(m\zeta)\ , \tag{2.23a}$$

$$g_m(\zeta) = \frac{\lambda_m\mu_3}{m\mu_b}\left[(-1)^{m/2} - \cos(m\zeta)\right]\ , \tag{2.23b}$$

$$\lambda_m = \frac{m^2 - v^2}{1-\mu}\ , \tag{2.23c}$$

$$m = 2,4,6,\ldots\ . \tag{2.23d}$$

Therefore, from Eqs. (2.20) and (2.23), we see that for the splay deformations the profile of the odd director modes is not influenced by the backflow and experiences an effective viscosity that does not depend either on the modal index or on the applied voltage; on the other hand, the even director modes get distorted by the backflow and are subject to an effective viscosity that generally depends both on the modal index and on the applied voltage.

The first proper mode whose decay constant λ_m, by increasing the applied voltage, becomes equal to zero defines the critical mode for a second-order Fréedericksz-type transition: it is characterized by a critical slowing down and is accompanied by a huge increase of its amplitude, while the corresponding velocity profile goes to zero. In our case this happens for the first splay mode even in the director profile for $v^2 = 1$ and $q_m = 1$, as one easily recognizes from Eqs. (2.20c) and (2.22), and it corresponds to the usual transversally homogeneous splay Fréedericksz transition. If the elastic anisotropy r is less than a critical value approximately equal to 0.303 [18,19], or higher if there is a flexoelectric coupling [20,11], another kind of second-order transition, characterized by a splay-twist deformation periodic in the transverse direction y, takes place at lower field values: in this work we are not concerned with this type of transitions.

For $v^2 < 1$ the decay constant λ_c of the critical mode and the corresponding normalized wave vector q_c depend on the backflow parameter μ, as shown in Fig. 1. From this figure it is apparent that, even for very high values of μ, the decay constant λ_c has a practically quadratic dependence on the applied voltage. A very good approximated analytical expression can then be obtained by expanding in power series Eqs. (2.20c) and (2.22) around the solution $v^2 = 1$, $q_m = 1$. At the first order one easily obtains

$$\lambda_c = \frac{1 - v^2}{1 - \left(1 - \frac{8}{\pi^2}\right)\mu}\ . \tag{2.24}$$

Even for $\mu = 0.9$ the maximum error that one commits using this equation is approximately equal to 1%: typically the backflow parameter μ is on the order of 0.3 and thus (2.24) can be safely used in analyzing the experimental data.

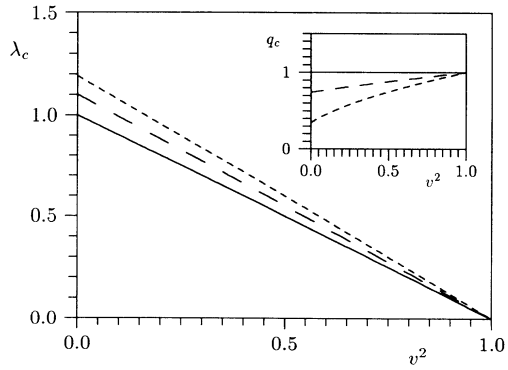

FIG. 1. Behavior of the normalized decay constant λ_c of the first splay mode as a function of the square of the normalized voltage v, for three different values of the backflow parameter: $\mu = 0$ (solid line), $\mu = 0.5$ (long-dashed line), and $\mu = 0.9$ (short-dashed line). The inset shows the corresponding values of the normalized wave vector q_c.

In thermodynamic equilibrium the splay modes even in the director profile can be represented as

$$n_z(\zeta,\tau;m)=\frac{d}{\pi}\sqrt{\frac{2k_BT}{\mathcal{V}K_1}}\,c_m(\tau)\left[\cos(q_m\zeta)-\cos(q_m\pi/2)\right]\,, \tag{2.25}$$

$\mathcal{V}$ being the volume of the cell, k_B Boltzmann's constant, and T the absolute temperature. The normalization constant in Eq. (2.25) has been chosen on grounds of convenience. The amplitudes $c_m(\tau)$ are Gaussian zero mean value stochastic variables whose correlation functions are given by [21]

$$\langle c_m(0)c_m(\tau)\rangle=\langle c_m^2\rangle\exp(-\lambda_m|\tau|)\,, \tag{2.26}$$

where $\langle\,\rangle$ indicates thermal average. The square mean values of these dynamic modes can be computed by making use of the even splay eigenvectors of the free energy operator (2.3)

$$n_z'(\zeta,\tau;m)=\frac{d}{\pi}\sqrt{\frac{2k_BT}{\mathcal{V}K_1}}\,b_m(\tau)\cos(m\zeta)\,,\qquad m=1,3,5,\dots\,, \tag{2.27}$$

whose amplitudes b_m, according to Eq. (2.1) and the equipartition theorem, are uncorrelated zero mean value Gaussian variables such that

$$\langle b_mb_n\rangle=\frac{\delta_{mn}}{m^2-v^2}\,, \tag{2.28}$$

δ_{mn} being the Kronecker delta. Then, by expanding at a given time the even splay director fluctuation modes in the bases of the static and dynamic fluctuation modes

$$\sum_m n_z'(\zeta,\tau;m)=\sum_m n_z(\zeta,\tau;m)\,, \tag{2.29}$$

and using the orthogonality of the static modes, we easily obtain

$$\langle c\,c^t\rangle=P^{-1}Q\left(P^{-1}\right)^t\,, \tag{2.30}$$

where c is the infinite column matrix containing the amplitudes c_m of the dynamic modes, P is the infinite square projection matrix whose elements P_{mn} are given by

$$\begin{aligned}P_{mn}&=\frac{2}{\pi}\int_{-\pi/2}^{\pi/2}\left[\cos(q_n\zeta)-\cos(q_n\pi/2)\right]\cos(m\zeta)\,d\zeta\\&=(-1)^{(m-1)/2}\,\frac{4q_n^2\cos(q_n\pi/2)}{m\pi\left(m^2-q_n^2\right)}\,,\qquad m=1,3,5,\dots\,,\end{aligned} \tag{2.31}$$

and finally Q is the infinite square diagonal matrix whose elements are given by Eq. (2.28). Equation (2.30) shows that in the presence of backflow the dynamic even splay modes become generally correlated.

A well approximated expression for the square mean value $\langle c_1^2\rangle$ of the amplitude of the critical dynamic mode can be obtained by retaining in the right hand side of Eq. (2.30) only the critical static mode

$$\langle c_1^2\rangle=\left[\frac{\pi\left(1-q_c^2\right)}{4q_c^2\cos(q_c\pi/2)}\right]^2\,\frac{1}{1-v^2}\,. \tag{2.32}$$

In a light-scattering experiment, the amplitude of the scattered electromagnetic field due to a given fluctuating mode is proportional to the Fourier transform of the director profile computed for a wave vector equal to the scattering optical wave vector [22]. Therefore in the case of forward nondepolarized scattering, i.e., for zero scattering wave vector, the amplitude of the scattered light due to the critical mode is proportional to

$$\begin{aligned}d_1&=\frac{c_1}{2}\int_{-\pi/2}^{\pi/2}\left[\cos(q_c\zeta)-\cos(q_c\pi/2)\right]d\zeta\\&=\left[\frac{\sin(q_c\pi/2)}{q_c}-\frac{\pi}{2}\cos(q_c\pi/2)\right]c_1\,,\end{aligned} \tag{2.33}$$

where the constant of proportionality has been chosen in such a way that $d_1=c_1$ in the absence of backflow ($\mu=0$). By using the approximated expression (2.32) and the first-order series expansion of Eq. (2.22) around the solution $v^2=1$, $q_m=q_c=1$, we then get

$$\langle d_1^2\rangle=\frac{1}{1-v^2}\,. \tag{2.34}$$

Equation (2.34) is confirmed by an exact numerical calculation based on Eq. (2.30), as shown in Fig. 2: the apparent increase of the intensity $\langle c_1^2\rangle$ of the critical mode when the backflow μ increases is actually mostly due to the fact that, as shown in the inset of Fig. 1, by increasing μ the wave vector q_c decreases, and so therefore does the maximum of the profile (2.20a). However, even for $\mu=0.9$ the maximum increase of the normalized scattered intensity $\langle d_1^2\rangle$, with respect to the value without backflow, is only about 1.5%.

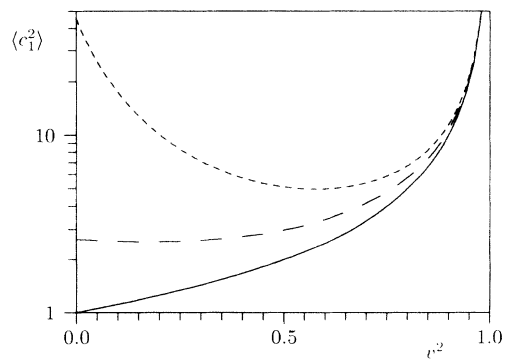

FIG. 2. Mean square value $\langle c_1^2\rangle$ of the amplitude of the first splay dynamic mode as a function of the square of the normalized voltage v for the same values of the backflow parameter μ as in Fig. 1. The corresponding normalized values of the scattered light intensity $\langle d_1^2\rangle$ [see Eq. (2.33)] cannot be graphically distinguished from the noise intensity in the absence of backflow (solid line curve).

III. EXPERIMENT AND RESULTS

The experimental setup used to detect the critical splay mode is shown in Fig. 3. The NLC cell is an 8.3 μm sample of 4-cyano-4'-*n*-pentylbiphenyl (K15 by British Drug House), having a positive dielectric anisotropy ϵ_a, with a strong planar anchoring obtained by a rubbed polyimide layer deposited on the indium tin oxide (ITO)-coated glass slides. The undistorted director and the polarization of the incident and scattered light lie in the scattering plane (plane of the figure). A 1 kHz ac voltage is supplied to the ITO cell electrodes by a signal generator. The external incidence and scattering angles, both measured with respect to the cell normal, are equal to $\alpha_{in} = \alpha_{out} = 40°$: this means that the photodiode used to detect the scattered light is placed in front of the transmitted beam, and it collects all the light coming from a cone having a semiaperture of about 0.1° centered about the transmitted beam's direction. The divergence of the laser beam is approximately equal to 0.06°. The extraordinary polarizations of the incoming and outgoing beams select only the splay fluctuation modes. In these conditions the detected scattered light is highly heterodyned and comes predominantly from the first dynamic splay mode: in fact the internal scattering wave vector is nearly equal to zero. The scattering cross section is proportional to the square sine of the sum of the internal incidence and scattering angles [22]: for this reason a nonnormal-incidence geometry was chosen. All the measurements were taken at a room temperature of (22 ± 1) °C.

The noise power spectrum of the detected signal is recorded through a digital fast Fourier transform (FFT) signal analyzer set at 10 Hz full scale and 100 averages, with a spectral resolution of 400 lines. Under our heterodyne conditions the power spectrum is proportional to the Fourier transform of the correlation function $\langle d_1(0)d_1(t)\rangle$ of the amplitude of the scattered signal d_1. Therefore, according to the results of Sec. II, up to a proportionality factor, it is very well approximated by the Lorentzian

$$S(\nu) = \frac{A}{1 + \left(\frac{\nu}{\Gamma}\right)^2}, \tag{3.1}$$

where ν is the frequency in hertz, A is the zero-frequency amplitude,

$$A = \left[1 - \left(\frac{V}{V_F}\right)^2\right]^{-2}, \tag{3.2}$$

V_F being the threshold of the splay Fréedericksz transition,

$$V_F = \pi\sqrt{\frac{K_1}{\epsilon_0\epsilon_a}}, \tag{3.3}$$

and finally Γ is the width, in hertz, of the Lorentzian,

$$\Gamma = \frac{\pi K_1}{2\eta d^2}\left[1 - \left(\frac{V}{V_F}\right)^2\right], \tag{3.4}$$

where η is the effective viscosity,

$$\eta = \gamma_1\left[1 - \left(1 - \frac{8}{\pi^2}\right)\mu\right]. \tag{3.5}$$

Figure 4 shows the variation of the linewidth Γ as a function of the square of the rms applied voltage V. The experimental points, obtained by a Lorentzian least squares fit of the noise spectra, show the predicted quadratic dependence on the applied voltage. The threshold voltage V_F obtained by the interpolation of these data is equal to 0.76 V and is in good agreement with other kinds of measurements [23,24]. Using the value of the dielectric anisotropy $\epsilon_a = 10.6$ reported in [25], we then obtain, according to Eq. (3.3), a value of the splay elastic constant of $K_1 = 5.5 \times 10^{-7}$ dyn. Then,

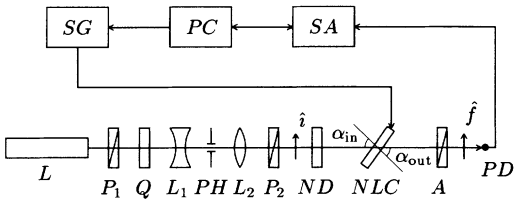

FIG. 3. Experimental setup. The polarizer P_1 and the quarter-wave plate Q act as an optical isolator of the light emitted by the 20 mW He-Ne laser L. The laser beam is spatially filtered and focused on the sample through the diverging lens L_1, the pin hole PH, and the converging lens L_2. The incoming $\hat{\imath}$ and outgoing $\hat{\mathbf{f}}$ polarizations of the light are determined by the polarizer P_2 and the analyzer A, respectively. The external incidence α_{in} and scattering α_{out} angles with respect to the normal to the planar sample NLC are equal. The undistorted nematic director lies in the scattering plane (plane of the drawing). The incident light is attenuated by a suitable neutral density filter ND and detected by the photodiode PD. A 1 kHz ac voltage is supplied to the cell by the signal generator SG controlled by the computer PC and the signal detected by the photodiode is amplified and sent to the digital FFT signal analyzer SA.

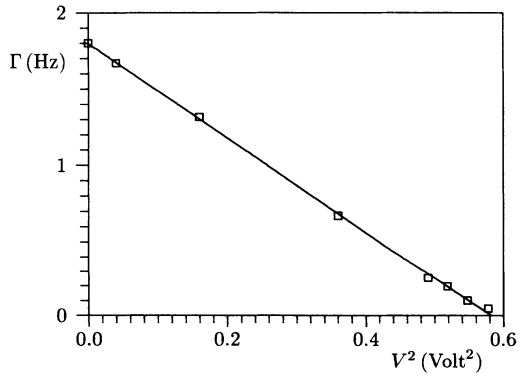

FIG. 4. Linewidth Γ of the Lorentzian spectra as a function of the square of the rms applied voltage V. The points are the experimental data, the solid line is a linear best fit.

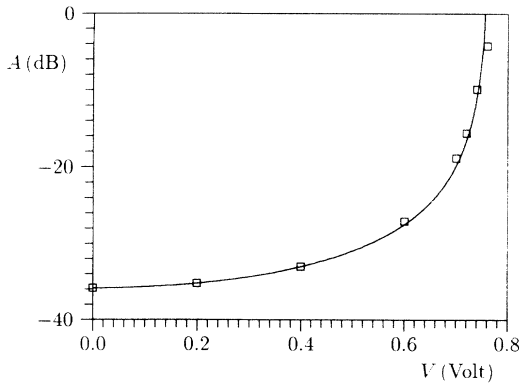

FIG. 5. Zero-frequency amplitude A of the Lorentzian spectra as a function of the rms applied voltage V. The points are the experimental data, the solid line is proportional to Eq. (3.2), with the threshold voltage $V_F = 0.76\,\mathrm{V}$ determined from the best fit of the linewidths.

using Eq. (3.4), and the zero-voltage linewidth $\Gamma(V = 0) = 1.8\,\mathrm{Hz}$, we get, for $d = 8.3\,\mu\mathrm{m}$, the effective viscosity $\eta = 70\,\mathrm{cP}$, that is compatible with the values of the viscosity coefficients reported in the literature [26].

Finally, Fig. 5 shows the zero-voltage amplitude A of the spectra as a function of the rms applied voltage V: the critical behavior predicted by Eq. (3.2) is confirmed. Of course the experimental points do not show a perfect divergence at the critical point, as the nonlinear corrections to the equations of motion limit the maximum fluctuation amplitude.

IV. CONCLUSIONS

We have theoretically analyzed the dynamics of the fluctuation modes that are homogeneous in the transverse directions in a NLC cell with strong planar anchoring in the presence of an electric field normal to the cell plates, determining their profile, decay constants, and fluctuation amplitudes in thermal equilibrium. We have shown that the presence of backflow alters the profile only of the even splay modes and we have obtained very well approximated expressions for the decay constant and the fluctuation amplitude of the critical mode, comparing them with exact numerical calculations.

We have then performed a direct measurement of the critical behavior of the first splay mode in the electrically induced splay Fréedericksz transition by analyzing the dynamics of the forward-scattered light in a nondepolarized scattering geometry. The experimental data show a very good agreement with the theoretical predictions and allow a high-accuracy determination of the critical fields without the need to apply fields that cause a finite static distortion. By knowing the dielectric anisotropy of the liquid crystal we have finally determined the splay elastic constant and the related effective viscosity.

[1] D. Langevin and M. A. Bouchiat, J. Phys. (Paris) **36**, 197 (1975).
[2] J. L. Martinand and G. Durand, Solid State Commun. **10**, 815 (1972).
[3] Orsay Liquid Crystal Group, Phys. Rev. Lett. **25**, 1361 (1969).
[4] I. Haller and J. D. Litster, Mol. Cryst. Liq. Cryst. **12**, 277 (1971).
[5] H. Fellner, W. Franklin, and S. Christensen, Phys. Rev. A **11**, 1440 (1975).
[6] D. C. Van Eck and W. Westera, Mol. Cryst. Liq. Cryst. **38**, 319 (1977).
[7] J. Papanek, Mol. Cryst. Liq. Cryst. **179**, 139 (1990).
[8] K. Eidner, M. Lewis, H. K. M. Vithana, and D. L. Johnson, Phys. Rev. A **40**, 6388 (1989).
[9] V. Fréedericksz and V. Zwetkoff, Phy. Z. Sowjetunion **6**, 490 (1934).
[10] B. Ya. Zel'dovich and N. V. Tabyrian, Zh. Eksp. Teor. Fiz. **81**, 1738 (1981) [Sov. Phys. JETP **54**, 922 (1981)].
[11] P. Galatola, C. Oldano, and M. Rajteri, Phys. Rev. E (to be published).
[12] G. Vertogen, Z. Naturforsch., Teil A **38**, 1273 (1983).
[13] R. S. Akopyan and B. Ya. Zel'dovich, Zh. Eksp. Teor. Fiz. **87**, 1660 (1984) [Sov. Phys. JETP **60**, 953 (1984)].
[14] F. M. Leslie, Q. J. Mech. Appl. Math. **19**, 357 (1966).
[15] O. Parodi, J. Phys. (Paris) **31**, 581 (1970).
[16] P. G. de Gennes, *The Physics of Liquid Crystals* (Clarendon Press, Oxford, 1974), p. 171.
[17] P. G. de Gennes, *The Physics of Liquid Crystals* (Clarendon Press, Oxford, 1974), p. 166.
[18] F. Lonberg and R. B. Meyer, Phys. Rev. Lett. **55**, 718 (1985).
[19] C. Oldano, Phys. Rev. Lett. **56**, 1098 (1986); E. Miraldi *et al.*, Phys. Rev. A **34**, 4348 (1986); W. Zimmermann and L. Kramer, Phys. Rev. Lett. **56**, 2655 (1986).
[20] J. P. Bobylev and S. A. Pikin, Zh. Eksp. Teor. Fiz. **72**, 369 (1977) [Sov. Phys. JETP **45**, 195 (1977)]; J. P. Bobilev, V. G. Chigrinov, and S. A. Pikin, J. Phys. (Paris) Colloq. **40**, C3-331 (1979).
[21] F. Sagués and F. Arias, Phys. Rev. A **38**, 5367 (1988).
[22] S. Chandrasekhar, *Liquid Crystals* (Cambridge University Press, Cambridge, England, 1980).
[23] P. Galatola, J. Phys. (Paris) II **2**, 1995 (1992).
[24] P. Allia, P. Galatola, C. Oldano, P. T. Valabrega, L. Trossi, and C. Aprato, Mol. Cryst. Liq. Cryst. **25**, 23 (1993).
[25] B. J. Frisken and P. Palffy-Muhoray, Phys. Rev. A **39**, 1513 (1988).
[26] W. W. Beens and W. H. de Jeu, J. Phys. (Paris) **44**, 129 (1983); H. Kneppe, F. Schneider, and N. K. Sharma, Ber. Bunsenges. Phys. Chem. **85**, 784 (1981).